

The impact of triangularity on plasma confinement: TCV experiments vs non-linear gyrokinetic modelling

A. Marinoni, S. Brunner, Y. Camenen, S. Coda, J.P. Graves, M. Jucker, X. Lapillonne,
A. Pochelon, O. Sauter, L. Villard and the TCV Team

*Ecole Polytechnique Fédérale de Lausanne (EPFL), Centre de Recherches en Physique des
Plasmas, Association Euratom-Confédération Suisse, CH-1015 Lausanne, Switzerland*

Introduction

In the past few years experimental results from the TCV tokamak have highlighted the impact of the flux surface shape on heat transport, in particular the stabilizing role of negative triangularity on electron heat transport [1]. This has motivated a theoretical study of the relationship between plasma microinstabilities and shape, performed with the non-linear gyrokinetic code GS2 [2], initial results of which are reported in this paper. Linear and non-linear electrostatic simulations are performed on the actual reconstructed equilibria, compared to experimental data and used to shed light on the details of the stabilizing and destabilizing effects on a microscopic scale.

Gyrokinetic modelling

Comparison with non-linear simulations

The simulations have been performed with the flux-tube code GS2, which solves the Vlasov-Maxwell system of equations as an initial value problem. The code employs a ballooning representation for the linear terms, solved implicitly, and an explicit flux tube domain treatment for the non-linear terms. The code can handle different ion species and collisions (a diffusion pitch-angle operator has been used for this work) and is fully electromagnetic, even though the simulations performed here are in the electrostatic limit owing to the low beta values in the experiments considered ($2\mu_0 < p > / B_0^2 \simeq 10^{-3}$). The simulations are performed with three kinetic species (electrons, deuterium and carbon as impurity), 16 to 32 energy grid points, 20 to 40 circulating particles pitch angles, 16 to 32 parallel modes. Our convergence studies indicate that at least 11 poloidal modes and 6 times as many radial modes are necessary to attain an accuracy of about 8% on the saturated heat flux. The simulations discussed in this paper have been performed with 15 poloidal modes and 85 radial modes. An initial equilibrium reconstruction to determine the plasma boundary was followed by a simulation with the PRETOR [3] transport code to derive the steady-state current profile, which was then provided in input to the CHEASE [4] equilibrium code to calculate the complete equilibria directly read by GS2. To isolate just the effect of plasma shape, the GS2 simulations have been per-

formed keeping fixed temperature and density profiles when comparing different triangularities.

The effect of the triangularity can be appreciated in Fig. 1, which compares the ratio between the experimental thermal diffusivities, reconstructed from a power balance analysis, of two TCV pulses and their simulated values at three radial points. The two experimental cases differ only in the triangularity being, respectively, -0.4 and 0.4 at the edge [1]. The non-linear simulations are performed in the collisionless limit. It can be seen that the reduction in transport with negative triangularity is qualitatively reproduced, but a satisfactory quantitative match is only obtained near the plasma edge. The smaller ratios

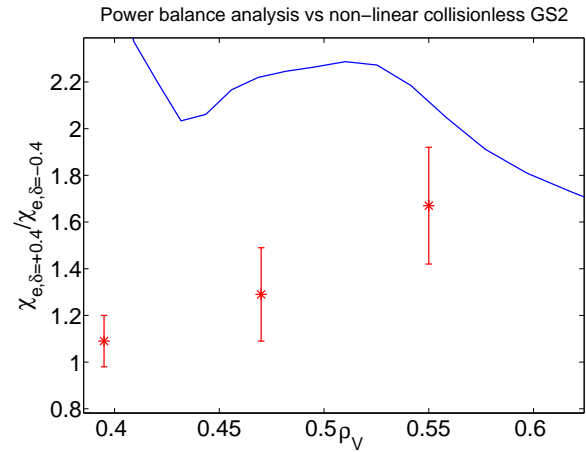


Figure 1: Solid curve: ratio of experimental electron thermal conductivities, as a function of the square root of the normalized volume, between discharges with edge triangularities equal to ± 0.4 . Red points: same ratio simulated by GS2: the mean values and their uncertainties are calculated in the saturated phase of the simulation.

ratios seen in the simulation towards the inside of the plasma might be explained by the finite penetration depth of triangularity. In particular, if at $\rho = 1$ the triangularities are ± 0.4 , at $\rho = 0.7$ they are equal to ± 0.17 and at $\rho = 0.4$ they are lower by a further factor of 3. Nevertheless the experimental diffusivity ratio is still about 2 even at the latter location. This observation may hint at global effects and cannot be explained by the present modelling. In the following all the numerical analysis is performed at $\rho = 0.7$. Another key experimental result is the linear scaling of the electron diffusivity with the inverse effective collisionality, irrespective of triangularity, as seen in Fig. 2a [1]. The same behaviour is roughly reproduced by the simulations (where the variation in collisionality is effected in practice by varying the density), with numerical values of the same order of magnitude of the experimental ones (Fig. 2b).

Investigation of instability drives

In fact the spectral region occupied by the most unstable modes and their propagation direction indicate that the dominant microinstability is the Trapped Electron Mode (TEM). This observation is confirmed in the non-linear simulations by the fact that the estimated saturated heat flux is carried primarily by the electron species. Additionally, the electron heat flux is mainly due to trapped particles, which confirms the TEM nature of the turbulence under investigation. This insight also works in favour of an intuitive explanation of the collisionality dependence observed in both simulations and experiments. In fact collisional detrapping processes alter the

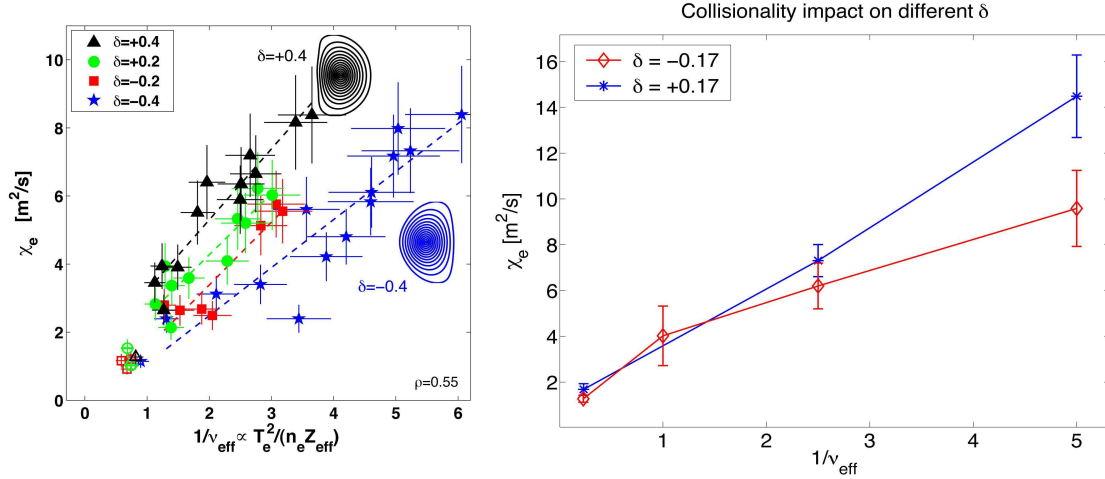


Figure 2: Effect of collisionality on the experimental (a: reprinted from [1]) and simulated (b) electron heat diffusivity. Since a) is calculated at $\rho = 0.55$ and b) at $\rho = 0.7$, the comparison is not meant as quantitative.

phase space configuration, leading to more and more particles being taken out of the highly unstable trapped region and transferred into the less unstable passing region, where they therefore contribute less to the overall transport. This is also reflected in a higher relative contribution of the passing electrons to the total (and decreased) calculated heat flux, as plotted in Fig. 3.

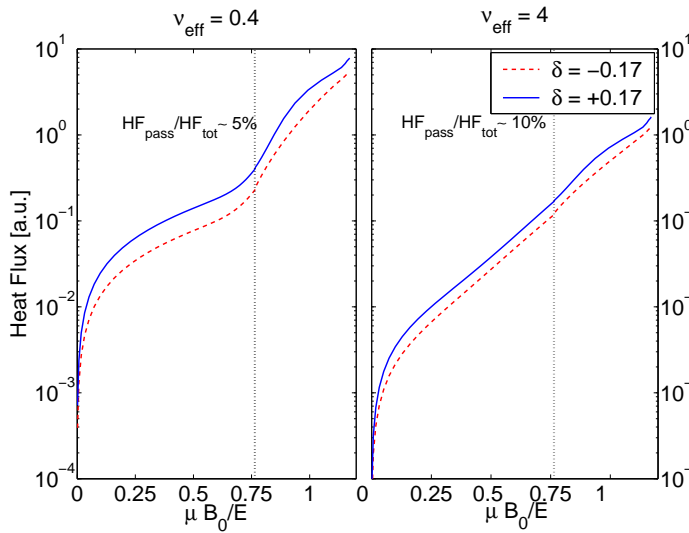


Figure 3: Heat Flux integrated over pitch angle against pitch angle for two values of collisionality. At higher v_{eff} the passing contribution to the total flux increases. Note how negative δ stabilizes also passing electrons, even though their contribution to the total flux is negligible.

The TEM was first theoretically investigated in [5], leading to the identification of the toroidal precession drift of trapped particles as the cause of the instability. Indeed, other parameters such as T_e/T_i and density and temperature scale lengths being equal, which is the case in the present experiments, it is natural to search for the cause of the observed dependence in the drifts induced by the magnetic topology. Even though the only operational difference between the TCV shots is the edge triangularity, this translates into differences in several quantities, both macroscopic, such as the Shafranov shift, and microscopic, such as the magnetic drifts. To understand how the different microscopic drifts interact, the positive triangularity case has been

Equil.	$\delta = 0.17$	$\delta = -0.17$	ω_d	$\omega_d + \nabla_{\perp}$	$\omega_d + \nabla_{//}$	∇_{\perp}	$\nabla_{\perp} + \nabla_{//}$	$\nabla_{//}$
χ_{ML}	1	0.77	0.90	0.74	0.92	0.82	0.84	0.98

Table 1: Heat Flux through mixing length estimate of real cases ($\delta = \pm 0.17$) and of artificially changed equilibria (all the others).

changed artificially by replacing one or more drives in the gyrokinetic equation, one at a time, with their corresponding values taken from the negative triangularity case. In particular, in the toroidal gyrokinetic equation one could isolate the effects of curvature and ∇B drifts (which have been simultaneously changed because they differ only in the negligible $\nabla\beta$ and are indicated as ω_d in Table 1), the parallel advection (indicated as $\nabla_{//}$ in Table 1) and the gradient of the ballooning eikonal, which reflects the effect of magnetic shear and can be interpreted as k_{\perp} (this parameter is indicated as ∇_{\perp} in Table 1 and has been changed independently of the perpendicular drifts for the sake of numerical investigation). The result of this linear test is depicted in Table 1 which reports the heat diffusivities, normalized to the positive triangularity case value, calculated through the generalization to general geometry of a mixing length estimate [6]. In particular it is evident that parallel and perpendicular dynamics behave differently: the curvature and ∇B drifts together with k_{\perp} act to reduce the linear growth rate of the perturbation in the negative δ case, whereas the parallel advection does not appreciably influence it. Even though these results are encouraging, it should be noted that this linear mixing-length estimate only gives a 30% difference in diffusivity between the two equilibria; nonlinear effects must therefore be paramount in accounting for the larger variation shown in Fig. 1. Other global effects not encapsulated yet in these reconstructed equilibria may also be at play.

Acknowledgements

The authors would like to thank Dr. Paolo Ricci for useful discussions, Dr. Trach-Minh Tran and Dr. Alberto Bottino for valuable assistance and the authors of the GS2 code for releasing the source. Simulations were performed on the Linux clusters PLEIADES and PLEIADES2 of the Ecole Polytechnique Fédérale de Lausanne. This work was supported in part by the Swiss National Science Foundation.

References

- [1] Y. Camenen, A. Pochelon et al., Nucl. Fusion **47** (2007) 510
- [2] M. Kotschenreuther, G. Rewoldt, W.M. Tang, Comput. Phys. Commun. **88** (1995) 128
- [3] D. Boucher and P.H. Rebut, Proc. IAEA Tech. Conf. on Advances in Simulation and Modeling in Thermonuclear Plasmas (Montreal, 1992) 142
- [4] H. Lütjens, A. Bondeson, O. Sauter, Comput. Phys. Commun. **97** (1996) 219
- [5] B.B. Kadomtsev and O.P. Pogutse, Zh. Eksp. Teor. Fiz. **51** (1966) 1734 [Sov. Phys. JETP **24** (1967) 1172]
- [6] F. Jenko et al., Plasma Phys. Controll. Fusion **47** (2005) B195